Application of a detailed biomass pyrolysis kinetic scheme to hardwood and softwood torrefaction

Andrés Anca-Couce[*,a], Ingwald Obernberger[a,b]

[a] Institute for Process and Particle Engineering, Graz University of Technology, Inffeldgasse 21b, 8010 Graz, Austria

[b] BIOS BIOENERGIESYSTEME GmbH, Inffeldgasse 21b, 8010 Graz, Austria

*anca-couce@tugraz.at, Tel.: +43 (0) 316 873-30432; Fax: +43(0) 316 873-1030432

Abstract

A detailed pyrolysis kinetic scheme is applied in this work for biomass torrefaction, with a focus on hardwood and softwood. The scheme includes secondary charring reactions, relevant for particles of a certain thickness, and sugar formation is avoided due to the catalytic effect of alkali metals in biomass. The release of acetic acid from hardwood and softwood hemicellulose is also considered. Representative initial compositions of hardwood and softwood are proposed in order to correctly predict mass loss in pyrolysis and torrefaction micro-TGA experiments. The predictions for product composition are validated with torrefaction batch experiments conducted in a lab-scale reactor with beech and spruce. The scheme predicts with good accuracy the yields of permanent gases and the main groups in which the condensable species are classified. The amount of secondary charring reactions is higher in the lab-scale than in the micro-TGA experiments, due to the higher particle size. The main discrepancies can be explained by the limitations of the scheme: reactive drying is not included and xylan is considered as representative for hemicellulose, which leads to deviations in the predictions of some products from softwood, e.g. furans. A more precise

description of hemicellulose from softwood would include a hemicellulose reaction scheme based on glucomannan.

Keywords: torrefaction, kinetic scheme, biomass, hardwood, softwood

1. Introduction

Biomass, as other renewable energy sources, is expected to play a more important role in the energy mix of the future. Torrefaction is a mild pyrolysis process at temperatures ranging from 220 to 350 °C where mainly the hemicellulose fraction decomposes. Torrefaction and its applications were reviewed by Van der Stelt et al. [1] and Tumuluru et al. [2]. In this process biomass loses mass and gets enriched in carbon due to volatiles release. Additionally, torrefaction improves grindability, increases hydrophobicity and reduces biological and thermal degradation, which improves storage and transportation properties. Due to these benefits torrefaction may become an interesting biomass pre-treatment technology.

Torrefaction is usually modelled with a two steps kinetic scheme [3, 4, 5] where there is at each step a competition between formation of volatiles and solid products. This scheme is inspired from the one developed for hemicellulose by Di Blasi and Lanzetta [6]. The composition of the volatiles of each reaction was calculated by Bates and Ghoniem [7] for a hardwood species (willow), based on the kinetics [3] and analysis of products [8] from Prins et al. The main limitation of this scheme is that it can just be applied for biomass species for which the kinetics and product composition were calculated, i.e. it cannot be generally applied for lignocellulosic biomass. Moreover, the competition between the production of char and volatiles is described with different activation energies for each reaction, not considering other relevant parameters in charring as particle size, pressure or ash content [9].

Biomass pyrolysis kinetics based on the sum of the contributions of the components hemicellulose, cellulose and lignin were also employed to describe mass loss in torrefaction [10, 11]. A kinetic scheme which is able to predict biomass pyrolysis should also be valid for biomass torrefaction, as this is just a partial pyrolysis process. The authors of this paper applied a detailed kinetic scheme of biomass pyrolysis [9, 12] to predict the product composition of torrefaction of beech (hardwood) chips [13]. The objective of this work is to present a general kinetic scheme which is able to generally predict mass loss evolution and product composition of torrefaction of lignocellulosic biomass. This kinetic scheme will be applied for hardwood and softwood torrefaction in this work. The kinetic scheme is presented in Section 2, mass loss evolution is discussed in Section 3 and product composition in Section 4. Finally, the conclusions are exposed.

2. Kinetic scheme

The pyrolysis kinetic scheme presented in this work to model biomass torrefaction is going to be briefly described. It is based on the scheme developed by Ranzi et al. [12] for pyrolysis of small ash free biomass particles (i.e., primary pyrolysis) called from now on original scheme. A recent update of this scheme, which has not been employed in this work, was presented by Corbetta et al. [14]. Biomass consists of cellulose, hemicellulose and 3 types of lignin which independently decompose and the volatiles are represented by 20 species, including main permanent gases and condensable species. This original scheme was adapted by the authors of this paper [9] to include the presence of secondary char formation reactions, which are relevant for particles of a certain thickness as under typical torrefaction conditions. In these reactions char is produced together with other products, such as H_2O and CO_2, from

the original products of primary pyrolysis. Moreover, in the competition between fragmentation and sugar formation reactions, the catalytic effect of alkali metals in biomass, together with the presence of secondary reactions of the volatiles in particles of a certain thickness, leads to the preference of the fragmentation pathway over sugar formation for both cellulose and hemicellulose in the adaptation.

The employed adapted scheme is summarized in Figure 1, the reactions are detailed in Table 1 and the list of species is shown in Table 2. Cellulose pyrolysis is described with one reaction representing devolatilization through ring fragmentation plus a secondary reaction representing charring. An adjustable parameter "x_1" represents the amount of the initial fragmentation primary products – $(Vol.+Char)_{1,1}$, including several low molecular weight compounds such as hydroxyacetaldehyde (HAA), 5-hydroxymethyl-furfural (HMFU), CO_2 or H_2O – that react to form the secondary products – $(Vol.+Char)_{2,1}$, including char, H_2O, CO_2 and H_2 –. The hemicellulose scheme is based on pyrolysis of xylan, which is a good representative of the hemicelluloses of hardwoods. It consists of two successive reactions. The scheme of lignin consists of three different components: LIG-C, LIG-H and LIG-O, which are richer in carbon, hydrogen and oxygen, respectively. Hemicellulose and lignin pyrolysis in the adapted scheme also include adjustable parameters "x_i" representing the amount of secondary charring reactions. These parameters should depend on the retention time and partial pressure of the volatiles in the particle, presence of minerals and temperature. A value in the range of 0.3–0.4, constant for all components, provided good results for slow pyrolysis in fixed beds of wood particles with a size of around 1 cm [9].

In this scheme char is not just produced as pure carbon, but also as several G{} forms (G{CO_2}, G{CO}, G{COH_2}) and G{H_2}) that further react at higher temperatures

producing CO_2, CO or H_2, but these reactions are not active at typical torrefaction temperatures.

Acetic acid is also included in the initial composition of hemicellulose from hardwoods and softwoods and it is released in the first hemicellulose reaction (R5). The main hemicellulose macromolecule of hardwoods is acetylglucuronoxylan [15], usually composed of 10 xylose molecules, 7 acetyl groups and 1 glucuronic acid [16]. The acetyl groups represent in this case around 15 % of the mass. In the original scheme hemicellulose is represented by xylan ($C_5H_8O_4$). In the adapted scheme, hardwood hemicellulose is represented by 10 xylan molecules ($C_5H_8O_4$) per 4 acetic acid ($C_2H_4O_2$, AA in Table 1 and Figure 1) ones, so that the acetic acid molecules represent around 15 % of the initial mass. The CHO (carbon, hydrogen and oxygen) contents of the new representative hemicellulose molecule (HCEHW) are almost not affected.

The hemicellulose scheme in the original Ranzi scheme is based on xylan, which is actually a better representative for hemicelluloses of hardwoods than softwood. Hemicellulose in softwood is composed of galactoglucomannan, glucomannan and arabinoglucuronoxylan [16, 17]. A reaction scheme based on glucomannan would be more appropriate for softwoods; however, it is not yet available. Hemicelluloses of softwoods are also acetylated, although to a lower extent than for hardwood. Glucomannan is usually composed of 4 hexose sugar monomers and 1 acetyl group [16]. The acetyl groups represent in this case around 4.5 % of the mass. In the adapted scheme, softwood hemicellulose (HCESW) is represented by 10 xylan molecules ($C_5H_8O_4$) per 1 acetic acid ($C_2H_4O_2$, AA in Table 1 and Figure 1), so that the acetic acid molecules represent around 4.5 % of the initial mass. However, the degree of

acetylation varies significantly for softwood [16], which can lead to uncertainties. The influence of employing xylan as a representative for softwoods will be later analysed.

It is proposed by the group of Ranzi to calculate the initial composition of each species based on the CHO contents provided by the elemental analysis [18]. But this approach is very sensitive to small experimental errors, as differences in CHO contents among biomass types are not large [19]. Therefore, another approach is followed here. A representative composition is taken for hardwood and softwood, shown in Table 3. These compositions will be employed for all simulations in this work. The mean value of the range reported in literature for lignin is selected [20]: 22% mass (18-25%) for hardwood and 30% mass (25-35%) for softwood. Cellulose content is set to 44% mass [20] for hardwood and softwood and the hemicellulose content is obtained by difference. The lignin composition (LIG-C, LIG-H and LIG-O) is calculated for the mean values for hardwood and softwood species reported by Faravelli et al. [21]. Softwood lignin is richer in LIG-C due to its higher carbon content.

3. Mass loss evolution

A general kinetic scheme should predict differences in pyrolysis and torrefaction of diverse biomass types. This work aims to predict the differences in mass loss between hardwood and softwood species. Hardwood and softwood have a different mass loss behaviour during pyrolysis, especially at low temperatures, which is very relevant for torrefaction. Gronli et al. [22] conducted micro thermo-gravimetric experiments at 5 K/min with initial masses of 5 mg of 4 hardwood and 5 softwood species. The adapted scheme is applied with the parameter "*x*", representing the amount of secondary charring reactions, equal to 0.2 in order to match the final char yield. This

parameter is lower than the value employed for pyrolysis of particles in the cm range at similar heating rates in typical fixed bed conditions (x = 0.3 – 0.4). The reason is the lower particle size, i.e., powder, in these micro-TGA experiments, which leads to less secondary charring reactions.

The scheme can correctly predict the mass loss evolution for hardwood and softwood species in these conditions, as seen in Fig. 2. The reaction rate at lower temperatures of softwoods is lower due to the lower hemicellulose content and differences in lignin composition. Softwood contains more LIG-C, which reacts at higher temperatures, and less LIG-H and LIG-O, which react at lower temperatures. The char yield of softwood is higher as lignin, especially LIG-C, produces more char.

As torrefaction is actually a partial pyrolysis process, a pyrolysis kinetic scheme should be also valid for torrefaction. The adapted kinetic is applied in Fig. 3 to predict torrefaction experiments conducted by Prins et al. [3] with willow (hardwood) at different temperatures. Experiments start at 200°C with a mass sample lower than 10 mg (powder) and the target temperature is achieved at a heating rate of 10 K/min; afterwards the temperature is kept constant. The model is applied with the parameter "x" equal to 0.2, as previously. Good agreement is found between the model and experimental results. The agreement is excellent for the torrefaction experiments at higher temperatures. The experimental mass loss starts slightly later than model predictions for the low temperature experiments. We can conclude that mass loss of lignocellulosic biomass torrefaction can be also predicted with this detailed kinetic scheme, although certain deviations are present at very low temperatures. Corbetta et al. [14] have already shown that the Ranzi scheme is able to predict mass loss evolution of cellulose, hemicellulose and lignin under torrefaction conditions.

4. Product composition

4.1 Experimental results

The product composition predicted by the scheme is going to be compared to experimental torrefaction results obtained with a batch lab-scale reactor. It consists of a cylindrical retort (0.35 m height and 0.12 m internal diameter) heated electrically by two separated PID controlled heating circuits. The biomass is put into a cylindrical holder (0.100 m height and 0.095 m i.d.) which is located inside the cylindrical retort. Nitrogen is introduced through a porous plate at the bottom of the fuel bed to keep the system inert and to remove the volatiles. A detailed explanation of the lab-scale reactor was given in a previous publication [23].

Torrefaction of beech chips at 250 and 285°C and of spruce chips at 250°C has been investigated. The initial bed weight was 190 g for beech and 75 g for spruce chips and the averaged particle sizes were 12 and 6 mm, respectively. Other properties are stated in Tab. 4. There is a good agreement between the experimental CHO contents and the ones employed in the model for hardwood and softwood (see Tab. 3 in comparison to Tab. 4). Each experiment was conducted two times in order to assure that there is repeatability. The relative deviation in the yields of the main groups that are presented in Tab. 5 is on average of ± 9%, related to the yield of each group. Temperatures were measured with thermocouples at different heights inside the bed. Since it was impossible to obtain a uniform temperature inside the bed, it has been decided to have the target torrefaction temperature at the middle of the bed. Heating rates in the order of 10 K/min were obtained and the target temperature was kept during approximately 20 minutes. Mass loss evolution and temperatures in the fuel bed are shown in Fig. 4. The detailed experimental results are available in [24] and results for beech woodchips were previously presented in [13].

Product composition is detailed in Tab. 5. Volatiles species are classified in permanent gases, light condensable species (LC) and heavy condensable species (HC). The torrgas is extracted from above the fuel bed and the concentrations of permanent gases (including CO, CO_2 and light hydrocarbons) as well as light condensable species were measured by Fourier transform infrared spectroscopy (FT-IR). H_2 was additionally measured by a heat capacity method. Light condensable species are water vapour and several oxygenated species with carbonyl and/or alcohol functional groups. Boiling points of these species range between -19°C for formaldehyde or 21°C for acetaldehyde to 118, 122 and 131 °C of acetic acid, lactic acid and hydroxyacetaldehyde, respectively.

In addition, heavy condensable species of the torrgas were measured using a gravimetric method (Tar protocol CEN TC BT/TF 290 143 WICSC 03002.4, 2005) as well as by gas chromatography (GC) coupled to mass spectrometry (MS) to identify the compounds and a flame ionization detector (FID) to quantify them (Agilent 6890N Network GC System). The tars were sampled in impinger bottles (filled with isopropanol) during the measurements and analysed afterwards in the laboratory. The detected compounds by GC-MS-FID were classified based on their structure in 4 different groups:

- Phenolic compounds: aromatic compounds with a phenyl group, such as guaiacols and syringols.
- (Hetero)cyclic compounds: cyclic compounds, mainly heterocyclics, such as furans (e.g. furfural).
- Carbonyl and/or alcohol compounds: not cyclic compounds with these functional groups, such as hydroxyacetone.
- Sugar compounds: mainly levoglucosan (LGA).

224 Boiling points of these species are higher than for light condensable species. Values
225 for hydroxyacetone and furfural are 146 °C and 162 °C, respectively. Phenolics,
226 sugars and other (hetero)cyclic compounds have even higher boiling points. The not
227 GC detected fraction of the gravimetric tars is assumed to be pyrolytic lignin [25] to
228 close the balance of gravimetric tars and it is included in the phenolics group. On the
229 contrary to pyrolysis, aromatics without oxygen content (BTX and PAH) are not
230 produced at these low temperatures.
231
232 *4.2 Model results*
233 The original Ranzi scheme [12], the adapted kinetic scheme presented in Section 2
234 and the two step kinetic scheme developed by Prins et al. [3] from experiments with
235 willow (hardwood), including the products of each reaction proposed by Bates and
236 Ghoniem [7] (named here Prins/Bates), are applied to describe the experiments. For
237 modelling purposes, the fuel bed is divided into three layers along the height of the
238 bed. The temperature evolutions have been measured for each layer (B1 for the top
239 layer - 90 mm from the bottom -; B2a, B2b and B2c for the middle layer - 50 mm
240 from the bottom and 25 mm from the centre for the radial ones - and B3 for the
241 bottom layer - 10 mm from the bottom -; see Fig. 4) and the evolutions of the layers
242 are modelled separately by the kinetic model. The entire fuel bed mass loss profile
243 and the final product composition are obtained by a mass weighted average of the
244 results of these three layers, assuming the same initial mass for all layers, as explained
245 in Mehrabian et al. [26]. The mass of initial humidity of biomass is included as water
246 vapour in the model predictions, together with the vapour released during torrefaction
247 of the dry biomass. The final product compositions obtained experimentally and by

248 the kinetic schemes are shown in Tab. 5 and Fig. 5. The adapted scheme is applied
249 with "*x*" equal to 0.3. The influence of this selection will be later analysed.
250 The final solid yield is reasonably well predicted by all schemes, considering that a
251 detailed model of heat and mass transfer in the bed is not employed. Slight over-
252 predictions may be caused by higher temperatures achieved near the heated walls than
253 in the position of the thermocouples. Radial temperatures are available for the middle
254 layer, but not for the bottom and top layers. However, significant differences are
255 present in the predictions of the main volatile groups. The original Ranzi scheme
256 predicts very high yields of the sugars levoglucosan and xylose, which leads to a
257 strong over-prediction of the total heavy condensable species. Levoglucosan is found
258 in the experiments, but in minor concentrations. This discrepancy is found because in
259 the original Ranzi scheme the catalytic effect of alkali metals during pyrolysis of
260 cellulose and hemicellulose, dramatically reducing the yields of sugars, is not
261 considered. Moreover, sugars can suffer secondary reactions in contact with char [9].
262 The experimental yields of sugars were actually lower for beech, with a higher ash
263 content and particle size. On the other hand, the yields of permanent gases, light
264 condensable species (including water vapour and the group of carbonyls and alcohols)
265 as well as (hetero)cyclic compounds are under-predicted by the original scheme.
266 These are main products of fragmentation reactions that are promoted over sugar
267 formation by alkali metals.
268 The adapted scheme significantly surpasses the other schemes. It has the best
269 predictions of the yields of permanent gases, light and heavy condensable species.
270 Yields of CO, CH_4 and other hydrocarbons are slightly over-predicted while the yield
271 of CO_2 is under-predicted. Regarding light condensable species, the adapted scheme
272 has an accurate prediction of the yield of carbonyls and alcohols due to their

formation in fragmentation reactions. Moreover, the yield of acetic acid from beech (hardwood) is correctly predicted due to the inclusion of the production of acetic acid from hemicellulose. The acetic acid yield from spruce (softwood) is however under-predicted. The prediction of the yield of water vapour is better than for the original scheme, as it is also produced in charring reactions, but remains under-predicted for all cases. Regarding heavy condensable species, it is corroborated by experiments that it is appropriate to eliminate sugar formation in these conditions, as previously discussed. The yield of (hetero)cyclics is well predicted for beech, but under-predicted for spruce; while the yield of phenolics is well predicted for all cases except for the high temperature case for beech.

The main discrepancies between the predictions of the adapted scheme and the experimental results can be explained by the limitations of the adapted scheme. Reactive drying, that takes place at around 200°C [2] and extractives are not included in the scheme. This may be the reason for the systematic under-prediction of the yields of water vapour, and probably also the one of CO_2. Hemicellulose is represented in this scheme by xylan, which is appropriate for hardwood. But glucomannan is the main component in hemicellulose from softwood, followed by galactoglucomannan and arabinoglucuronoxylan [27]. Despite the not correct approximation of employing xylan as representative hemicellulose species for softwood, the results for spruce are quite accurate. It was however previously noted that the yields of acetic acid and (hetero)cyclics were under-predicted for this case. Hardwood hemicellulose is strongly acetylated. Softwood hemicellulose is also acetylated, although in a lower proportion [28] and the degree of acetylation varies significantly [16], leading to a higher error. Moreover, a heterocyclic compound (HMFU) is reported to be a main product of softwood hemicellulose but it is not

298 produced from hardwood hemicellulose [29, 30]. A more precise description of
299 hemicellulose from softwood would improve the results further. The interactions
300 between biomass components are neither considered in the scheme [31], but this does
301 not seem to hinder significantly its ability to describe torrefaction as the sum of the
302 contributions of cellulose, hemicellulose and lignin. The effects of inorganics are
303 considered to some extent and the presented results are only valid for woody biomass.
304 The Prins/Bates scheme under-predicts the yields of permanent gases and, especially
305 of heavy condensable species. Heavy condensable species, as phenolics and furans,
306 are produced in significant amounts [32] but are disregarded in many torrefaction
307 studies, as in [8, 31]. This scheme predicts correctly the yields of water vapour and
308 carbonyls and alcohols, but under-predicts the yields of CO and CO_2. Moreover, it has
309 the limitations previously expounded in Section 1; it cannot be generally applied for
310 lignocellulosic biomass and charring is just a function of the temperature program, not
311 considering other relevant parameters.
312 Torrefied biomass samples were collected after the experiments from the three layers
313 along the height of the bed and thermo-gravimetric experiments of the samples were
314 conducted under nitrogen at 20 K/min with an initial mass of 50 mg until a final
315 temperature of 500°C. The volatile fractions corresponding to cellulose, hemicellulose
316 and lignin have been determined with a fitting routine in the figure plotting the
317 reaction rate ($d\alpha/dt$, being α conversion) over temperature (see Fig. 3 and Fig. 4 of
318 Brostrom et al. [33]). Pyrolysis is modelled with a parallel reaction scheme with 3
319 components representing the devolatilization of cellulose, hemicellulose and lignin.
320 Cellulose and hemicellulose conversion are calculated for each sample, related to the
321 contents of the original biomass, and are plotted in Fig. 6 as a function of the
322 maximum temperature seen by the sample in the lab-scale reactor. The adapted model

323 can correctly predict the conversion process of hemicellulose at temperatures around
324 250°C and the beginning of conversion of cellulose at around 300°C. There is just an
325 experimental outlier for hemicellulose conversion at the bottom of the bed for the
326 285°C experiment with beech, but it is probably caused because higher temperatures
327 are achieved near the heated wall than in the centre of the bed where the
328 thermocouple is placed.
329 Finally, the influence of variations of the "*x*" parameter on the predictions of the
330 adapted model is checked in Fig. 7 for the experiment with beech at 250°C. "*x*" is
331 kept constant for all reactions in all cases. When it increases, the yield of total solids
332 and water vapor also increases, as these are the main products of charring reactions.
333 On the other hand, the yields of permanent gases, carbonyls and alcohols,
334 (hetero)cyclics and phenolics decrease, as these are the main reactants of the charring
335 reactions. The minimum averaged error is obtained for "*x*" equal to 0.3 and 0.4 (1.0%
336 error in both cases). Therefore, as for fixed bed pyrolysis, a value in this range is
337 recommended for biomass torrefaction in a fixed bed with particles of around 1 cm
338 and slow heating rates (around 10K/min). Different values for each component can
339 potentially offer a better description of the process, but there is not enough
340 information available for setting the optimal value for each component currently. The
341 mass loss micro-TGA experiments that have been presented in Section 3 have been
342 modelled with a "x" parameter of 0.2. A higher parameter is required to model the
343 lab-reactor experiments due to the higher extent of secondary charring. Moreover,
344 even though slow heating rates have been employed in the lab-scale experiments,
345 intra-particle gradients can be present due to the endothermic drying, heat transfer
346 limitations during the heat-up phase and exothermic reactions afterwards [34]. The
347 "x" parameter may to some extent include these phenomena. A more detailed

description of the bed of particles would include intra and inter-particle heat and mass transfer phenomena.

5. Conclusions and recommendations

A detailed kinetic scheme able to generally predict mass loss evolution and product composition of torrefaction of lignocellulosic biomass is presented in this work. It is a pyrolysis scheme that has been applied in this work to torrefaction, which is actually a partial pyrolysis process. It considers secondary char formation reactions, which are relevant for particles of a certain thickness, and the catalytic effect of alkali metals which avoids sugar formation. Representative initial compositions of hardwood and softwood are proposed and the release of acetic acid from hardwood and softwood hemicellulose is included. The scheme correctly predicts mass loss in micro-TGA pyrolysis and torrefaction experiments and product composition in torrefaction experiments done in a batch lab-scale reactor with beech and spruce. The "x" parameter, representing the amount of secondary charring, is set to 0.2 for the micro-TGA experiments. A higher value, in the range from 0.3 to 0.4, is required to describe the fixed bed torrefaction experiments in the lab-scale reactor with particles of woody biomass in the cm range at slow heating rates (around 10 K/min), due to the higher particle size employed in these experiments. Products of torrefaction are classified in permanent gases, light and heavy condensable species. Moreover, the condensable species are classified according to their structure in five groups: carbonyls and alcohols, water vapour, (hetero)cyclics, sugars and phenolics. The scheme predicts with good accuracy the yields of these groups and the main discrepancies can be explained by the limitations of the scheme. Reactive drying at around 200°C is not included, so the water vapour yield is under-predicted. Moreover, the hemicellulose

scheme is based on xylan, which leads to inaccuracies for softwood, such as the under-prediction of the yield of furan compounds. A more precise description of hemicellulose from softwood would include a hemicellulose reaction scheme based on glucomannan and a more precise description of the degree of acetylation. Future work could include the application of the reaction scheme to non woody biomass species and the combination of the detailed reaction scheme with the description of intra and inter-particle heat and mass transfer in a bed of particles.

6. References

(1) van der Stelt MJC, Gerhauser H, Kiel JHA, Ptasinski KJ. Biomass & Bioenergy **2011**, 35 (9), 3748-3762.

(2) Tumuluru JS, Sokhansanj S, Hess JR, Wright CT, Boardman RD. Industrial Biotechnology **2011**, 7 (5), 384-401.

(3) Prins MJ, Ptasinski KJ, Janssen FJJG. Journal of Analytical and Applied Pyrolysis **2006**, 77 (1), 28-34.

(4) Repellin V, Govin A, Rolland M, Guyonnet R. Biomass & Bioenergy **2010**, 34 (5), 602-609.

(5) Ren SJ, Lei HW, Wang L, Bu Q, Chen SL, Wu J. Biosystems Engineering **2013**, 116 (4), 420-426.

(6) DiBlasi C, Lanzetta M. Journal of Analytical and Applied Pyrolysis **1997**, 40, 287-303.

(7) Bates RB, Ghoniem AF. Bioresource Technology **2012**, 124, 460-469.

(8) Prins MJ, Ptasinski KJ, Janssen FJJG. Journal of Analytical and Applied Pyrolysis **2006**, 77 (1), 35-40.

(9) Anca-Couce A, Mehrabian R, Scharler R, Obernberger I. Energy Conversion and Management **2014**, 87, 687-696.

(10) Turner I, Rousset P, Remond R, Perre P. International Journal of Heat and Mass Transfer **2010**, 53 (4), 715-725.

(11) Tapasvi D, Khalil R, Várhegyi G, Tran KQ, Grønli M, Skreiberg O. Energy & Fuels **2013** 2013, 27, 6134−6145

(12) Ranzi E, Cuoci A, Faravelli T, Frassoldati A, Migliavacca G, Pierucci S and Sommariva S. Energy & Fuels **2008**, 22, 4292-4300.

(13) Anca-Couce A, Mehrabian R, Scharler R, Obernberger I. Chemical Engineering Transactions **2014**, 37, 43-48.

(14) Corbetta M, Frassoldati A, Bennadji H, Smith K, Serapiglia MJ, Gauthier G, Melkior T, Ranzi E, Fisher EM. Energy & Fuels **2014**, 28 (6), 3884-3898.

(15) Moreira LRS, Filho EXF. Applied Microbiology and Biotechnology 2008, 79 (2), 165-178.

(16) Patil RA. Cleavage of Acetyl Groups for Acetic Acid Production in Kraft Pulp Mills. Electronic Theses and Dissertations, paper 1857, University of Maine, 2012.

(17) Spiridon I, Popa, V. Hemicelluloses: Major Sources, Properties and Applications, in: Belgacem, M.N., Gandini, A. (Eds.), Monomers, Polymers and Composites from Renewable Resources. Elsevier, Oxford, England, 2008.

(18) Cuoci A, Faravelli T, Frassoldati A, Granata S, Migliavacca G, Ranzi E, Sommariva S. Proceedings of the 30th Combustion Meeting of the Italian Section of the Combustion Institute VI **2007**, 2.1-2.6.

(19) Vassilev SV, Baxter D, Andersen LK, Vassileva CG. Fuel **2010**, 89 (5), 913-933.

(20) Wagenfuhr R, C. Scheiber C. Holzatlas, Leipzig Fachbuchverlag, 1974.

(21) Faravelli T, Frassoldati A, Migliavacca G and Ranzi E. Biomass & Bioenergy **2010**, 34, 290-301.

(22) Gronli MG, Varhegyi G, Di Blasi C. Industrial & Engineering Chemistry Research **2002**, 41, 4201-4208.

(23) Brunner T, Biedermann F, Kanzian W, Evic N, Obernberger I. Energy & Fuels **2013**, 27 (10), 5691–5698.

(24) Anca-Couce A, Brunner T, Obernberger I. Proceedings of the 23rd European Biomass Conference & Exhibition, 1035 - 1041. 1-4 June 2015. Vienna.

(25) Scholze B, Meier D. Journal of Analytical and Applied Pyrolysis **2001**, 60, 41–54.

(26) Mehrabian R, Anca-Couce A, Scharler R, Obernberger I, Janisch W, Trattner K. Proceedings of the 21st European Biomass Conference & Exhibition, 879 - 886. 3-7 June 2013, Copenhagen. ISSN: 2282-5819.

(27) Branca C, Di Blasi C, Mango C, I. Hrablay I. Industrial & Engineering Chemistry Research **2013**, 52 (14), 5030-5039.

(28) Candelier K, Chaouch M, Dumarcay S, Petrissans A, Petrissans M, Gerardin P. Journal of Analytical and Applied Pyrolysis **2011**, 92 (2), 376-383.

(29) Di Blasi C, Branca C, Galgano A. Industrial & Engineering Chemistry Research **2010**, 49 (6), 2658-2671.

(30) Raisanen U, Pitkanen I, Halttunen H, Hurtta M. Journal of Thermal Analysis and Calorimetry **2003**, 72 (2), 481-488.

(31) Nocquet T, Dupont C, Commandre JM, Grateau M, Thiery S, Salvador S. Energy **2014**, 72, 188–194.

(32) Zheng AQ, Zhao ZL, Chang S, Huang Z, He F, Li HB. Energy & Fuels **2012**, 26 (5), 2968-2974.

(33) Brostrom M, Nordin A, Pommer L, Branca C, Di Blasi C. Journal of Analytical and Applied Pyrolysis 2012, 96, 100-109.

(34) Bates RB, Ghoniem AF. Fuel 2014, 137, 216–229.

Table 1: List of reactions of the adapted scheme (SW: softwood, HW: hardwood).

Reaction				A [s^{-1}]	E [kJ/mol]
1	CELL	→	$(1-x_1)$ * (0.95 HAA + 0.25 GLYOX + 0.2 CH_3CHO + 0.25 HMFU + 0.2 C_3H_6O + 0.16 CO_2 + 0.23 CO + 0.9 H_2O + 0.1 CH_4 + 0.61 Char) + x_1 * (5.5 Char + 4 H_2O + 0.5 CO_2 + H_2)	8×10^{13}	192.5
5	HCE	→	0.4 * [$(1-x_5)$ * (0.75 $G\{H_2\}$ + 0.8 CO_2 + 1.4 CO + 0.5 CH_2O + 0.25 CH_3OH + 0.125 ETOH + 0.125 H_2O + 0.625 CH_4 + 0.25 C_2H_4 + 0.675 Char) + x_5 * (4.5 Char + 3 H_2O + 0.5 CO_2 + H_2)] + 0.6 HCEA2	1×10^{10}	129.7
5 (HW)	HCEHW	→	0.4 AA + 0.4 * [$(1-x_5)$ * (0.75 $G\{H_2\}$ + 0.8 CO_2 + 1.4 CO + 0.5 CH_2O + 0.25 CH_3OH + 0.125 ETOH + 0.125 H_2O + 0.625 CH_4 + 0.25 C_2H_4 + 0.675 Char) + x_5 * (4.5 Char + 3 H_2O + 0.5 CO_2 + H_2)] + 0.6 HCEA2	1×10^{10}	129.7
5 (SW)	HCESW	→	0.1 AA + 0.4 * [$(1-x_5)$ * (0.75 $G\{H_2\}$ + 0.8 CO_2 + 1.4 CO + 0.5 CH_2O + 0.25 CH_3OH + 0.125 ETOH + 0.125 H_2O + 0.625 CH_4 + 0.25 C_2H_4 + 0.675 Char) + x_5 * (4.5 Char + 3 H_2O + 0.5 CO_2 + H_2)] + 0.6 HCEA2	1×10^{10}	129.7
8	HCEA2	→	$(1-x_8)$ * (0.2 CO_2 + 0.5 CH_4 + 0.25 C_2H_4 + 0.8 $G\{CO_2\}$ + 0.8 $G\{COH_2\}$ + 0.7 CH_2O + 0.25 CH_3OH + 0.125 ETOH + 0.125 H_2O + Char) + x_8 * (4.5 Char + 3 H_2O + 0.5 CO_2 + H_2)	1×10^{10}	138.1
9	LIG-C	→	0.35 LIG-CC + 0.1 pCOUMARYL + 0.08 PHENOL + 0.41 C_2H_4 + H_2O + 0.495 CH_4 + 0.32 CO + $G\{COH_2\}$ + 5.735 Char	4×10^{15}	202.9
10	LIG-H	→	LIG-OH + C_3H_6O	2×10^{13}	156.9
11	LIG-O	→	LIG-OH + CO_2	1×10^{9}	106.7
12	LIG-CC	→	$(1-x_{12})$ * (0.3 pCOUMARYL + 0.2 PHENOL + 0.35 $C_3H_4O_2$ + 0.7 H_2O + 0.65 CH_4 + 0.6 C_2H_4 + $G\{COH_2\}$ + 0.8 $G\{CO\}$ + 6.4 Char) + x_{12} * (14.5 Char + 3 H_2O + 0.5 CO_2 + 4 H_2)	5×10^{6}	131.8
13	LIG-OH	→	H_2O + CH_3OH + 0.45 CH_4 + 0.2C_2H_4 + 1.4 $G\{CO\}$ + 0.6 $G\{COH_2\}$ + 0.1 $G\{H_2\}$ + 4.15 Char + [$(1-x_{13})$ * (y_{13}/100 * FE2MACR + (1 - y_{13}/100) * (H_2O + 0.5 CO + 0.2 CH_2O + 0.4 CH_3OH + 0.2 CH_3CHO + 0.2 C_3H_6O + 0.6 CH_4 + 0.65 C_2H_4 + $G\{CO\}$ + 0.5 $G\{COH_2\}$ + 5.5 Char)) + x_{13} * (10.5 Char + 3 H_2O + 0.5 CO_2 + 3 H_2)]	3×10^{8}	125.5
			y_{13} = - 3.6800E-11 * T^5 + 8.2619E-08 * T^4 - 6.8901E-05 * T^3 + 2.6124E-02 * T^2 - 4.5911 * T + 4.0398E+02; T in [°C]		
16	$G\{CO_2\}$	→	CO_2	1×10^{5}	100.4
17	$G\{CO\}$	→	CO	1×10^{13}	209.2
18	$G\{COH_2\}$	→	CO + H_2	5×10^{11}	272.0
19	$G\{H_2\}$	→	H_2	5×10^{11}	313.8

453 **Table 2:** List of species.

Abbreviation	Name	Atomic composition	Group
Solids			
CELL	Cellulose	$C_6H_{10}O_5$	
HCE	Hemicellulose	$C_5H_8O_4$	
HCEHW	Hemicellulose for hardwoods	10 * ($C_5H_8O_4$) + 4 *($C_2H_4O_2$)	
HCESW	Hemicellulose for softwoods	10 * ($C_5H_8O_4$) + 1 *($C_2H_4O_2$)	
HCEA2	Activated hemicellulose 2	$C_5H_8O_4$	
LIG-C	Carbon-rich lignin	$C_{15}H_{14}O_4$	
LIG-H	Hydrogen-rich lignin	$C_{22}H_{28}O_9$	
LIG-O	Oxygen-rich lignin	$C_{20}H_{22}O_{10}$	
LIG-CC	Carbon-rich lignin 2	$C_{15}H_{14}O_4$	
LIG-OH	OH-rich lignin	$C_{19}H_{22}O_8$	
G{CO_2}	Trapped CO_2	CO_2	
G{CO}	Trapped CO	CO	
G{COH_2}	Trapped COH_2	CH_2O	
G{H_2}	Trapped H_2	H_2	
Char	Char	C	
Volatiles			
AA / HAA	Acetic acid / Hydroxyacetaldehyde	$C_2H_4O_2$	Carbonyls + alcohols
GLYOX	Glyoxal	$C_2H_2O_2$	Carbonyls + alcohols
C_3H_6O	Propanal (Acetone)	C_3H_6O	Carbonyls + alcohols
$C_3H_4O_2$	Propanedial	$C_3H_4O_2$	Carbonyls + alcohols
HMFU	5-hydroxymethyl-furfural	$C_6H_6O_3$	Furans
LVG	Levoglucosan	$C_6H_{10}O_5$	Sugars
XYL	Xylose monomer	$C_5H_8O_4$	Sugars
pCOUMARYL	Paracoumaryl alcohol	$C_9H_{10}O_2$	Phenolics
PHENOL	Phenol	C_6H_6O	Phenolics
FE2MACR	Sinapaldehyde	$C_{11}H_{12}O_4$	Phenolics
H_2	Hydrogen	H_2	Permanent gases
CO	Carbon monoxide	CO	Permanent gases
CO_2	Carbon dioxide	CO_2	Permanent gases
CH_4	Methane	CH_4	Permanent gases
CH_2O	Formaldehyde	CH_2O	Carbonyls + alcohols
CH_3OH	Methanol	CH_4O	Carbonyls + alcohols
C_2H_4	Ethylene	C_2H_4	Permanent gases
CH_3CHO	Acetaldehyde	C_2H_4O	Carbonyls + alcohols
ETOH	Ethanol	C_2H_6O	Carbonyls + alcohols
H_2O	Water vapour	H_2O	Water vapour

454

455

Table 3: Modeled composition of hardwood and softwood in ash-free % mass.

	Hardwood	Softwood
Cellulose	44.0	44.0
Hemicellulose	34.0	26.0
LIG-C	6.0	17.5
LIG-H	7.0	9.5
LIG-O	9.0	3.0
Total lignin	22.0	30.0
% C	48.6	51.0
% H	6.0	6.0
% O	45.4	43.0

459 **Table 4:** Elemental analysis, ash and moisture content of employed fuels.

	Beech chips (Hardwood)	Spruce chips (Softwood)
C (% mass d.b.)	48.44	50.14
H (% mass d.b.)	6.03	6.16
O (% mass d.b.)	44.46	43.22
N (% mass d.b.)	0.12	0.06
Ash (% mass d.b.)	0.95	0.42
Moisture (% mass w.b.)	6.4	5.2

460

461

Table 5: Experimental (exp.) and model product compositions (original, adapted with x = 0.3 and Prins/Bates schemes) in mass percentage of initial wet biomass (w.t.%). LC: light condensable species, HC: heavy condensable species.

	Spruce 250°C				Beech 250°C				Beech 285 °C			
	Exp.	Orig.	Adap. x=0.3	Prins/ Bates	Exp.	Orig.	Adap. x=0.3	Prins/ Bates	Exp.	Orig.	Adap. x=0.3	Prins/ Bates
Solid												
Total solid	77.96	82.24	83.29	84.82	71.68	74.07	74.73	77.92	58.01	61.99	63.90	66.15
Permanent gases												
Hydrogen	0.17	0.00	0.06	0.00	0.15	0.00	0.09	0.00	0.12	0.00	0.15	0.00
Carbon monoxide	1.08	0.64	1.23	0.36	1.01	0.79	1.57	0.44	1.65	1.14	2.03	0.63
Carbon dioxide	4.32	1.08	2.08	1.76	4.94	2.10	3.42	2.14	6.46	2.85	4.67	3.07
Methane	0.08	0.53	0.59	0.00	0.13	0.73	0.76	0.00	0.41	1.11	1.07	0.00
Ethylene	0.02	0.48	0.50	0.00	0.01	0.63	0.60	0.00	0.00	0.96	0.84	0.00
Propane	0.00				0.01				0.03			
Propene	0.00				0.29				0.56			
Total permanent gas	5.66	2.72	4.46	2.12	6.54	4.25	6.44	2.57	9.22	6.07	8.75	3.70
Water vapour (LC)												
Total water vapour	9.10	5.88	7.17	9.21	12.46	7.35	9.26	11.64	16.15	8.03	11.46	14.55
Carbonyls + alcohols (mainly LC)												
Formaldehyde	0.67	0.89	0.87		0.28	1.38	1.20		0.32	2.09	1.63	
Acetaldehyde	0.00	0.00	0.06		0.01	0.00	0.13		0.06	0.01	0.40	
Propanal (Acetone)	0.00	0.81	0.89		0.00	0.63	0.79		0.01	0.72	1.24	
Methanol	0.27	0.56	0.58	0.85	0.53	0.91	0.87	2.07	0.86	1.40	1.26	4.38
Ethanol	1.45	0.27	0.28		1.25	0.41	0.39		1.97	0.62	0.52	
Hydroxyacetaldehyde (Acetic acid)	1.56	0.00	1.00	1.54	4.22	0.01	3.93	2.42	6.08	0.05	6.19	4.21
Glyoxal		0.00	0.10			0.00	0.21			0.01	0.66	
Propanedial		0.00	0.00			0.00	0.00			0.00	0.00	
Lactic acid	0.39			0.62	0.27			1.85	0.39			4.14
Formic acid	0.00			0.54	0.00			0.89	0.04			1.60
Hydroxyacetone (HC)				0.21				0.52				1.11
GC detected (HC)	0.58				0.51				0.94			
Total carbonyls + alcohols	4.93	2.52	3.79	3.75	7.09	3.34	7.51	7.76	10.67	4.90	11.89	15.44
(Hetero)cyclics (HC)												
Furfural				0.09				0.11				0.16
5-hydroxymethyl-furfural (HMF)		0.00	0.23			0.01	0.45			0.03	1.43	
GC detected	0.57				0.64				1.29			
Total furans	0.57	0.00	0.23	0.09	0.64	0.01	0.45	0.11	1.29	0.03	1.43	0.16
Sugars (HC)												
Levoglucosan	0.28	1.61	0.00		0.06	3.15	0.00		0.10	9.61	0.00	0.00
Xylose monomer		3.62	0.00			5.60	0.00			5.81	0.00	0.00
Total sugars	0.28	5.23	0.00	0.00	0.06	8.76	0.00	0.00	0.10	15.42	0.00	0.00
Phenolics (HC)												
Paracoumaryl alcohol		0.16	0.16			0.09	0.09			0.14	0.14	
Phenol		0.08	0.08			0.04	0.04			0.07	0.07	
Sinapaldehyde		1.16	0.82			2.10	1.48			3.34	2.35	
GC detected	0.44				0.91				1.80			
Not GC detected	1.06				0.61				2.77			
Total phenolics	1.50	1.40	1.06	0.00	1.53	2.23	1.61	0.00	4.56	3.56	2.57	0.00

List of figure captions:

Figure 1: Summary of the adapted reaction scheme. The release of acetic acid (AA) from hemicellulose is different for hardwood and softwood.

Figure 2: Experiments [22] and model predictions of reaction rates (top, dY/dt, being $Y = m/m_0$, m mass and t time) and mass loss (middle) over temperature of pyrolysis at 5 K/min with hardwood (left) and softwood (right) species. The evolution of cellulose, hemicellulose, lignin, char and G{} forms predicted by the model is shown at the bottom.

Figure 3: Experiments [3] and model predictions for torrefaction of willow (hardwood) at different temperatures.

Figure 4: Mass loss and temperature evolution in the fuel bed during the batch lab-scale torrefaction experiments.

Figure 5: Product composition of the main groups and species in mass percentage of initial wet biomass.

Figure 6: Cellulose and hemicellulose conversion as a function of the maximum temperature seen by the sample in the lab-scale reactor. Model results obtained with the adapted scheme and "x" = 0.3 for all components.

Figure 7: Comparison of the predictions of the adapted model with different ''x'' values, constant for all reactions in each case, based on the experiments with beech at 250°C.

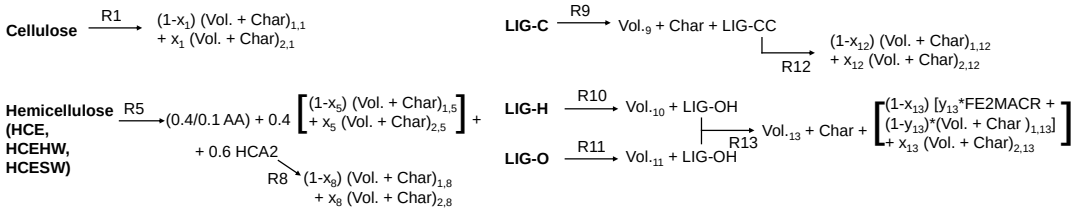

Figure 1: Summary of the adapted reaction scheme. The release of acetic acid (AA) from hemicellulose is different for hardwood and softwood.

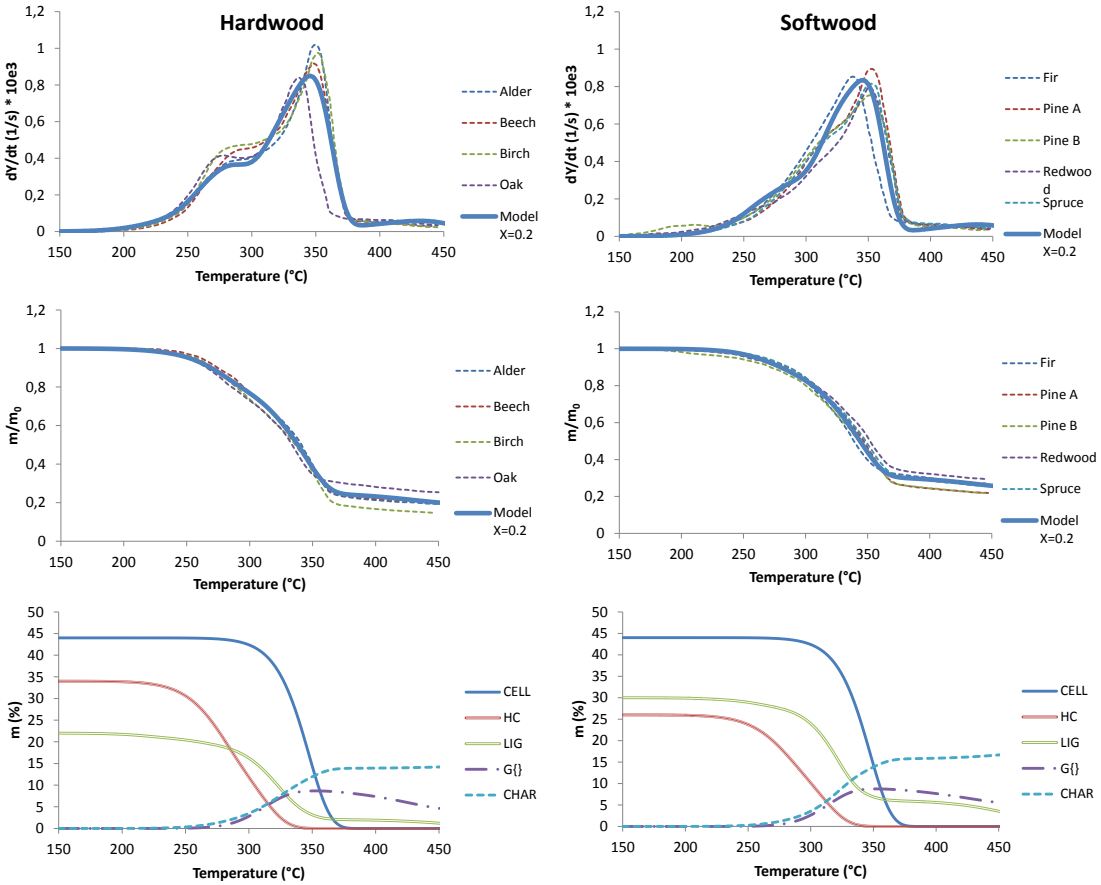

Figure 2: Experiments [22] and model predictions of reaction rates (top, *dY/dt*, being $Y = m/m_0$, m mass and t time) and mass loss (middle) over temperature of pyrolysis at 5 K/min with hardwood (left) and softwood (right) species. The evolution of cellulose, hemicellulose, lignin, char and G{} forms predicted by the model is shown at the bottom.

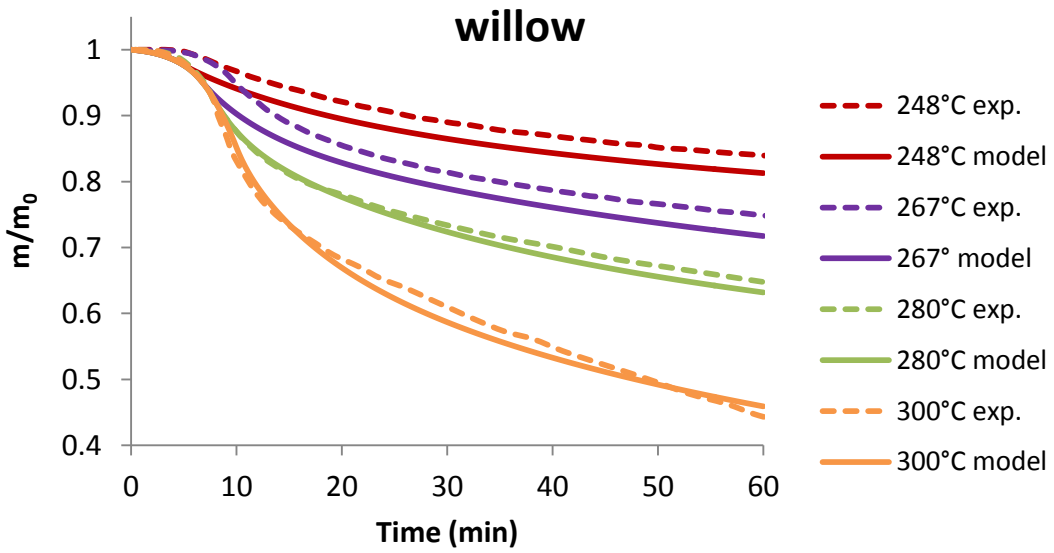

497

498 **Figure 3:** Experiments [3] and model predictions for torrefaction of willow

499 (hardwood) at different temperatures.

500

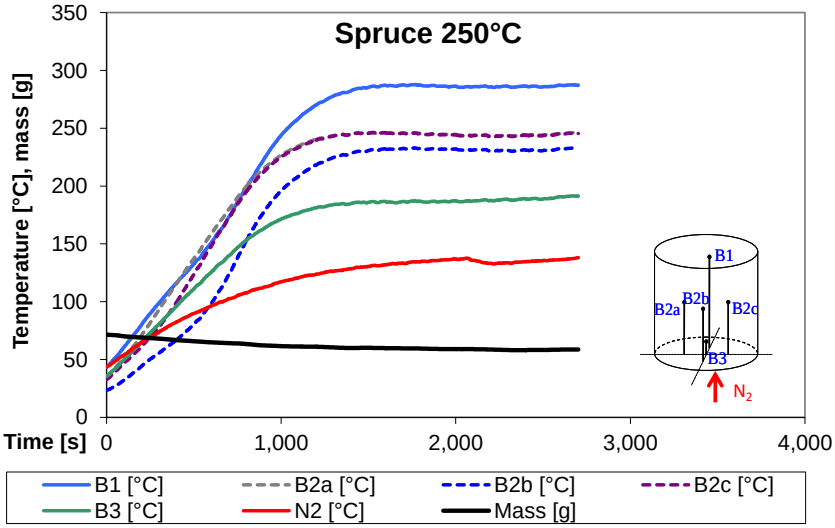

501

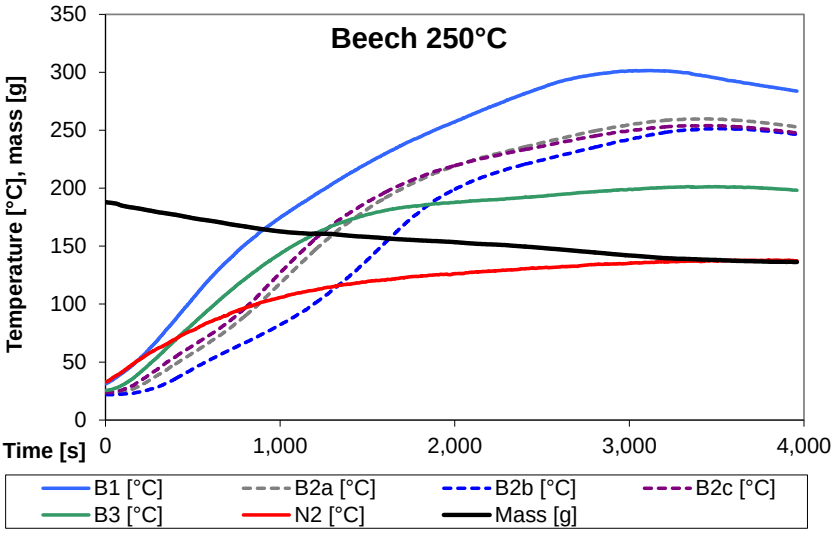

502

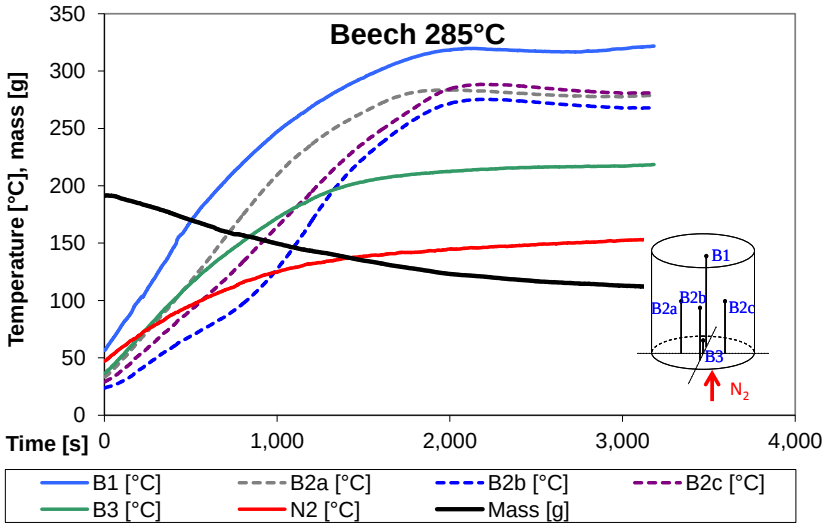

503

504 **Figure 4**: Mass loss and temperature evolution in the fuel bed during the batch lab-

505 scale torrefaction experiments.

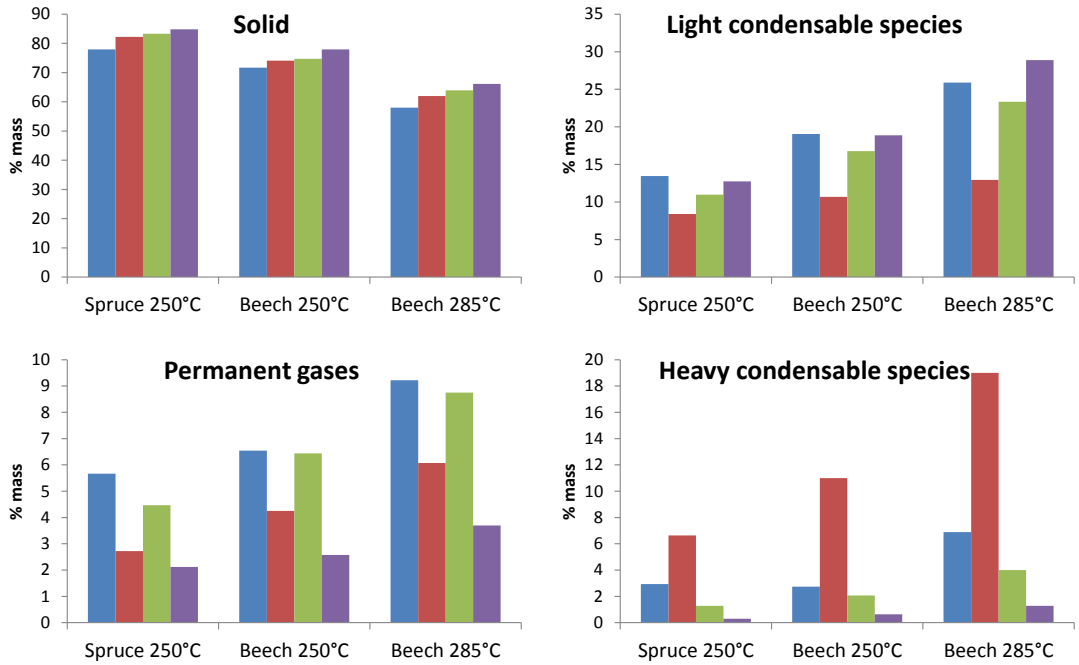

506

507 **Figure 5 (1/2)**: Product composition of the main groups and species in mass

508 percentage of initial wet biomass.

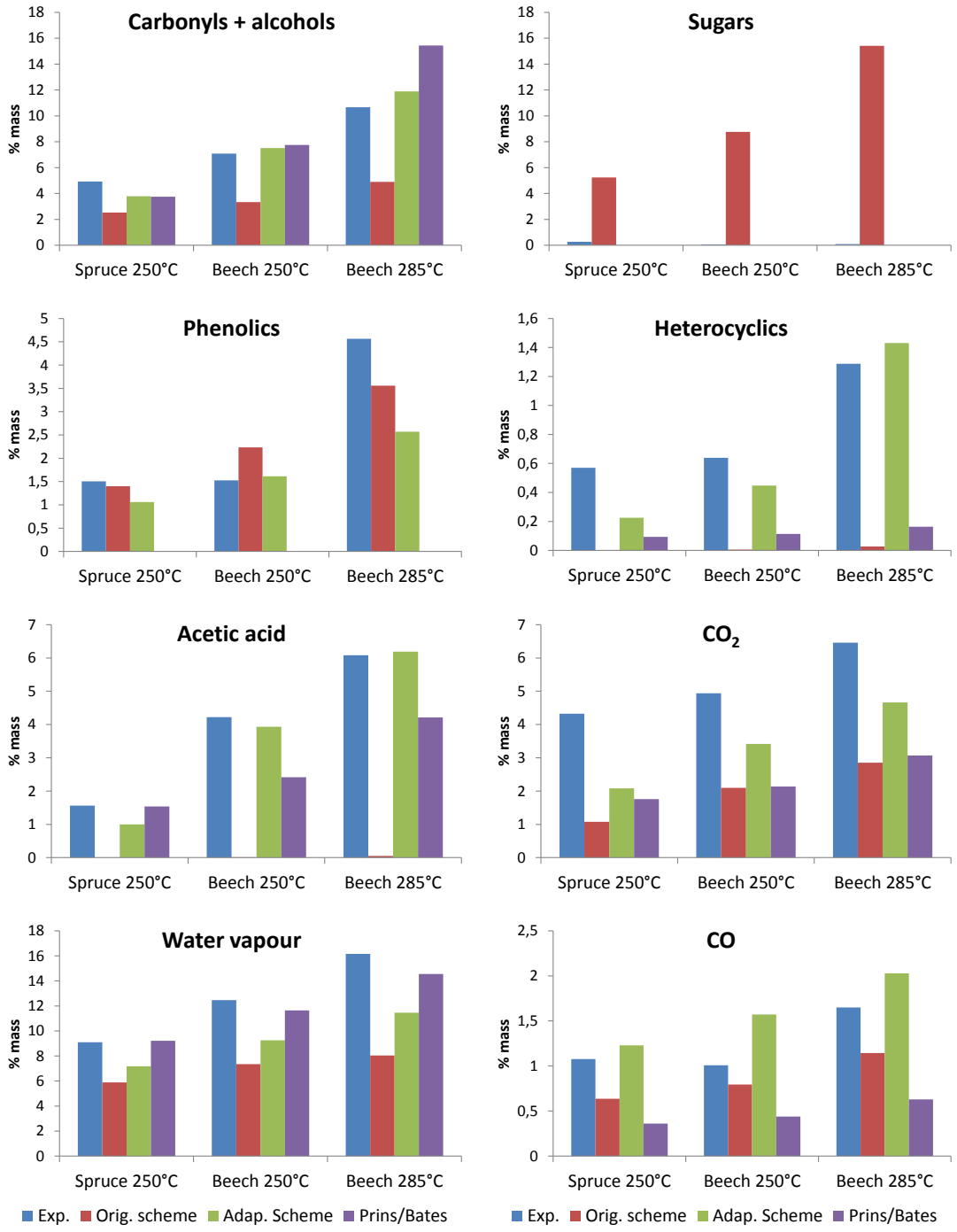

509

510 **Figure 5 (2/2)**: Product composition of the main groups and species in mass

511 percentage of initial wet biomass.

512

513

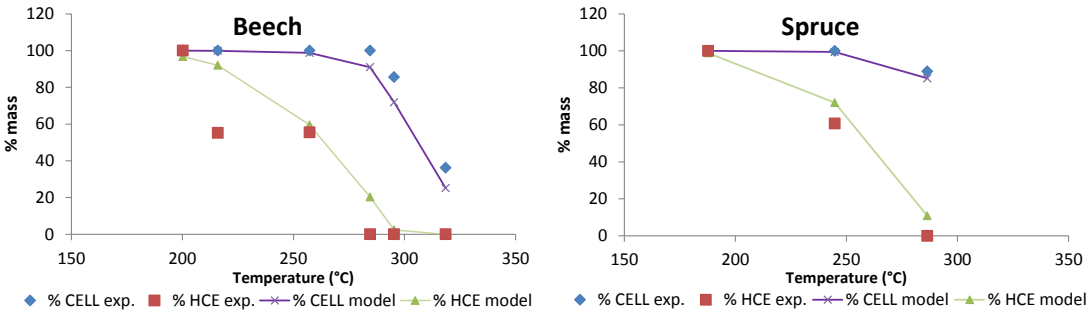

514

515 **Figure 6:** Cellulose and hemicellulose conversion as a function of the maximum
516 temperature seen by the sample in the lab-scale reactor. Model results obtained with
517 the adapted scheme and "*x*" = 0.3 for all components.

518

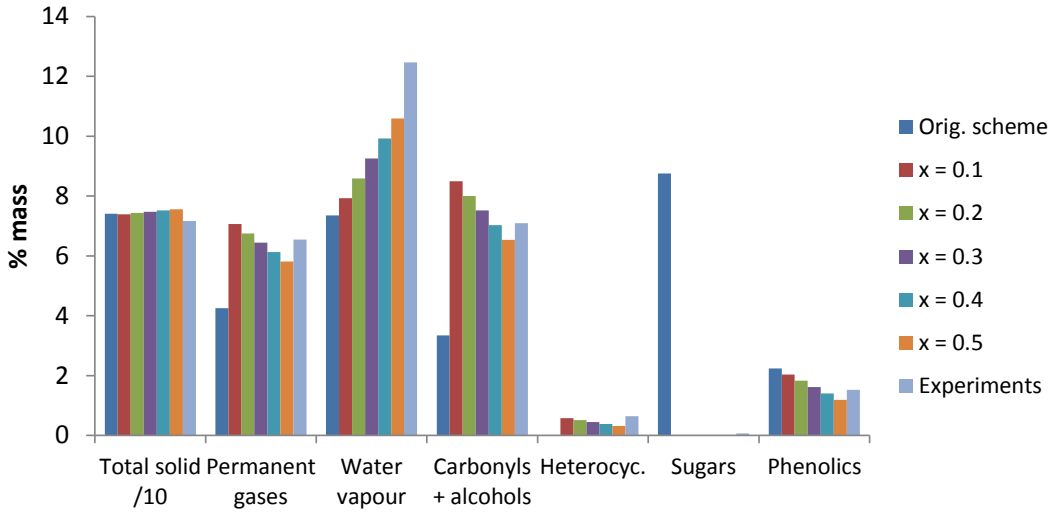

519

520 **Figure 7:** Comparison of the predictions of the adapted model with different ‘‘*x*’’

521 values, constant for all reactions in each case, based on the experiments with beech at

522 250°C.